

Angle-resolved photoemission spectroscopy of band tails in lightly doped cuprates

A. S. Alexandrov and K. Reynolds
Department of Physics, Loughborough University,
Loughborough LE11 3TU, United Kingdom

We amend *ab initio* strongly-correlated band structures by taking into account the band-tailing phenomenon in doped charge-transfer Mott-Hubbard insulators. We show that the photoemission from band tails accounts for sharp "quasi-particle" peaks, rapid loss of their intensities in some directions of the Brillouin zone ("Fermi-arcs") and high-energy "waterfall" anomalies as a consequence of matrix-element effects of disorder-localised states in the charge-transfer gap of doped cuprates.

PACS numbers: 71.38.-k, 74.40.+k, 72.15.Jf, 74.72.-h, 74.25.Fy

Since the discovery of high- T_c superconductivity in cuprates, angle-resolved photoemission spectroscopy (ARPES) has offered a tremendous advance into the understanding of their electronic structure [1]. However, even though ARPES is continually strengthening our insights into the band structure and correlations in cuprates, it has also revealed many poorly understood phenomena, such as the incoherent "background", the sharp "quasi-particle" peaks near some points of the Brillouin zone (BZ), which form "arcs" of "Fermi surface" (FS) ([2] and references therein), widely studied low-energy dip-hump and kink features (for review see [1]) and the more recently discovered steep downturn of the dispersion toward higher energies (the so-called "waterfall") [3, 4, 5, 6, 7, 8, 9]. These anomalies have received quite different interpretations, involving, for example, uncorrelated [11] and strongly-correlated [3, 12, 13, 14, 15] lattice polarons, Migdal-Eliashberg-like approaches [16, 17], spinons and holons [4], spin polarons [6], spin fluctuations [10, 18] and band-structure matrix element effects [9, 19].

Many ARPES interpretations suggest a large FS (as an exception see e.g. [11]) with nodal gapless quasiparticles, which are gapped or strongly damped in the antinodal directions $((0,0) \rightarrow (\pi,0))$ of the two-dimensional (2D) BZ. Importantly, extensive simulations of ARPES using the first-principles (LDA) band theory with the matrix elements properly taken into account [19] reproduces well the topological features of momentum distribution curves (MDC), pointing to the large FS in optimally doped cuprates. However, LDA predicts that the undoped parent cuprates are metallic with roughly the same large FS, while they are actually charge-transfer Mott-Hubbard insulators with the optical gap at 2 eV. This fact led to several powerful extensions of LDA, in particular to LDA+U, which combines LDA eigenfunctions with strong Coulomb correlations introduced as a model parameter (Hubbard U) [20], and the LDA+generalized tight-binding (GTB) method combining the exact diagonalization of the intracell part of the Hamiltonian with relevant LDA eigenfunctions and Coulomb correlations and the perturbation treatment of the intercell hoppings and interactions [21]. LDA-GTB Hamiltonian is reduced

to the simpler effective $t - J$ or $t - J^*$ model ($t - J$ model plus three-center correlated hoppings [21]) in the low-energy domain.

LDA+GTB band structure of undoped cuprates with *ab initio* sets of tight-binding parameters [21] describes remarkably well the optical gap, $E_{ct} \approx 2$ eV both in antiferromagnetic and paramagnetic states of the undoped La_2CuO_4 . The valence band consists of a set of very narrow ($\lesssim 1$ eV) subbands where the highest one is dominated by the oxygen p states with the maximum at $\mathbf{k} \equiv \mathbf{g} = (\pi/2a, \pi/2a)$ (see Fig.1), while the bottom of the empty conduction band formed by $d_{x^2-y^2}$ states of copper is found at $(\pi/a, 0)$. These locations of valence-band maximum and conduction-band minimum perfectly agree with ARPES intensity locus in hole doped $\text{La}_{2-x}\text{Sr}_x\text{CuO}_4$ and electron-doped $\text{Nd}_{2-x}\text{Ce}_x\text{CuO}_4$, respectively [22]. Importantly, the LDA+GTB approach predicts the charge-transfer gap at any doping with the chemical potential pinned near the top of the valence band (in hole doped cuprates) and near the bottom of the conduction band (in electron-doped cuprates) due to spin-polaron *in-gap* states.

ARPES of undoped cuprates [1, 2, 3, 22, 23, 24] proved to be critical in the assessment of different theoretical approaches. It revealed an apparent contradiction with the $t - J$ model. There is no sharp peak predicted by the model in undoped cuprates, but a slightly dispersive broad incoherent background, Fig.2 (inset). Small lattice polarons due to a strong electron-phonon interaction (EPI) have been advocated as a plausible explanation of the discrepancy [13]. When EPI is strong, the spectral weight, Z , of the coherent small-polaron peak is very small, $Z \ll 1$ and, hence the peak can not be seen in experiment since all weight of the sharp resonance in the $t - J$ model is transformed at strong EPI into the broad continuum.

Unfortunately the energy distribution curves (EDC) in La_2CuO_4 , Fig.2a, has only little if any resemblance to the small-polaron spectral function, which is roughly gaussian-like. Only by subtracting a "background" given by the spectrum near $(\pi/a, \pi/a)$, Fig.2a, one can account for the remaining EDC with the polaronic spectral function [15]. This background problem obscures any reli-

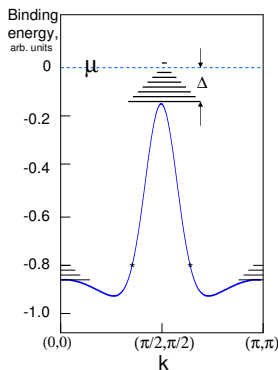


FIG. 1: LDA+GTB valence band dispersion [21] amended with band tails (ladder lines) near Γ , $(\pi/2, \pi/2)$ and (π, π) maxima (here k is measured in $1/a$)

able interpretation of the broad ARPES intensities, especially in underdoped cuprates, where the charge-transfer gap at 2 eV makes inelastic scattering events implausible as an explanation of the background. Sharp peaks at $(\pi/2a, \pi/2a)$ near the Fermi level, Fig.2b, in doped cuprates also remains a puzzle. Small heavy polarons cannot screen EPI in lightly doped cuprates. Hence, if Z is small in the parent cuprate, it should also remain small at finite doping, so that the emergency of the peaks cannot be explained by a substantial increase of Z with doping.

Here we show that amending the LDA+GTB band structure of doped cuprates by inevitable impurity band-tails, the ARPES puzzles as mentioned above are explained.

Doping of cuprates inserts a large number of impurities into the parent lattice. Each impurity ion locally introduces a distinct level, E_i , in the charge-transfer gap. The fact that the impurities are randomly distributed in space causes the density of states (DOS) to tail, like in heavily doped semiconductors [25]. When there are many impurities within the range ξ_i of a localised wave function $\psi_i(\mathbf{r})$, the random potential produces low-energy states near maxima of the valence band at hole doping, Fig.1, or near minima of the conduction band at electron doping. As a result, ARPES intensity, $I(\mathbf{k}, E) = I_b(\mathbf{k}, E) + I_{im}(\mathbf{k}, E)$ comprises the band-tail intensity, $I_{im}(\mathbf{k}, E)$, due to localised states within the charge-transfer gap, and the valence band contribution, $I_b(\mathbf{k}, E)$, of itinerant Bloch-like states. According to LDA band structures [19] the itinerant states are anisotropic-3D (specifically in La_2CuO_4) dispersing with c -axis k_z over a few hundred meV. We suggest that this dispersion shapes the background making it so different from the incoherent background caused by EPI and/or spin fluc-

tuations since k_z is not conserved in ARPES experiments. On the other hand the incoherent background can be well described by a simple polaronic Gaussian in presumably more anisotropic insulating $\text{Ca}_2\text{CuO}_2\text{Cl}_2$ [24].

Here we focus on the band-tailing contribution described by the Fermi-Dirac golden rule as

$$I_{im}(\mathbf{k}, E) = \frac{2\pi e^2}{m_e^2} n(E) \sum_i |\langle \psi_f | \mathbf{A}_0 \cdot \nabla | \psi_i \rangle|^2 \delta(E + \Delta - E_i). \quad (1)$$

We define all energies relative to the chemical potential, μ , which is situated within the impurity band as shown in Fig.1. Only the impurity states with the binding energy E_i below $\mu = 0$ contribute at zero temperature. Here \mathbf{A}_0 is the amplitude of X-ray vector potential, and $\hbar = k_B = 1$.

We take the impurity wavefunction as [26], $\psi_i(\mathbf{r}) = F_i(\mathbf{r})\psi_{\mathbf{g}}(\mathbf{r})$, and the final state to be the normalised plane wave, $\psi_f(\mathbf{r}) = (Nv)^{-1/2} \exp(i\mathbf{k} \cdot \mathbf{r})$. Here $\psi_{\mathbf{g}}(\mathbf{r})$ is the itinerant state at the top of the valence band, $F_i(\mathbf{r})$ is a slowly varying envelope function, and N is the number of unit cells of volume v in the crystal. In the framework of GTB [21] one can expand $\psi_{\mathbf{g}}(\mathbf{r})$ using the Wannier orbitals, $\psi_{\mathbf{g}}(\mathbf{r}) = N^{-1/2} \sum_{\mathbf{m}} w(\mathbf{r} - \mathbf{m}) \exp(i\mathbf{g} \cdot \mathbf{m})$, and calculate the dipole matrix element in Eq.(1) as

$$I_{im}(\mathbf{k}, E) = I_n(E) \sum_i |f_i(\mathbf{k} - \mathbf{g})|^2 \delta(E + \Delta - E_i), \quad (2)$$

where $I = 2\pi(ed/m_e)^2(\mathbf{A}_0 \cdot \mathbf{k})^2/v$ is proportional to the valence band matrix element squared, which is roughly a constant in a wide range of \mathbf{k} near \mathbf{g} , $d = \int d\mathbf{r} w(\mathbf{r}) \exp(i\mathbf{g} \cdot \mathbf{r})$, and $f_i(\mathbf{q}) = (Nv)^{-1} \int d\mathbf{r} \exp(i\mathbf{q} \cdot \mathbf{r}) F_i(\mathbf{r})$ is the Fourier transform of the impurity envelope function.

Since the size of the envelope is large compared with the lattice constant, its Fourier transform strongly depends on \mathbf{q} , which explains the experimental EDC and MDC as we show in the rest of the paper. We choose the impurity state to be hydrogen-like, $F_i(\mathbf{r}) = (Nv/\pi\xi_i^3)^{1/2} \exp(-r/\xi_i)$ as the hydrogen model accurately predicts many properties of shallow levels in heavily doped semiconductors, so that $f_i(\mathbf{q}) = 8\pi(\xi_i^3/\pi Nv)^{1/2}(1+q^2\xi_i^2)^{-2}$ for 3D impurity states, and $f_i(\mathbf{q}) \propto (1+q^2\xi_i^2)^{-3/2}$ for 2D states like localised surface states. It is important to recognise here that ξ_i is related to the impurity binding energy as $\xi_i^{-2} = mE_i$, where m is roughly the hole effective mass. As a result we get $I_{im}(\mathbf{k}, E) = xIn(E)M(\mathbf{k} - \mathbf{g}, E)$ with

$$M(\mathbf{k} - \mathbf{g}, E) = \frac{64\pi}{vm^{3/2}} \frac{(E + \Delta)^{5/2}}{[E + \Delta + (\mathbf{k} - \mathbf{g})^2/m]^4} \rho_{im}(E + \Delta). \quad (3)$$

Here $\rho_{im}(E) = N_i^{-1} \sum_i \delta(E - E_i)$ is the band-tail density of states (DOS) normalised to unity, and $x = N_i/N$ is the impurity concentration per cell proportional to doping. In the 2D case the result is similar, $M_{2D}(\mathbf{k}, E) \propto (E + \Delta)^2 [E + \Delta + (\mathbf{k}_{\parallel} - \mathbf{g})^2/m]^{-3} \rho_{im}(E + \Delta)$.

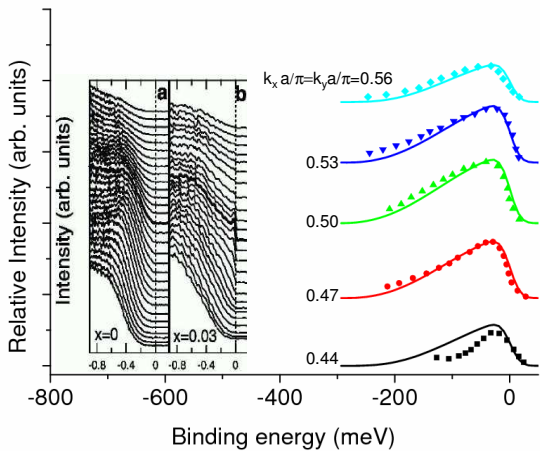


FIG. 2: Band-tail EDC, Eq.(4), (solid lines) with pseudogap $\Delta = 300$ meV and band-tail width $\gamma = 300$ meV compared with relative EDC (symbols) near $(\pi/2a, \pi/2a)$. Relative intensities are obtained by subtracting ARPES intensities of the parent compound, La_2CuO_4 (a), shifted by $\delta\mu$, from EDC of slightly doped $\text{La}_{1.97}\text{Sr}_{0.03}\text{CuO}_4$ (b) as measured by Yoshida *et al.* [2]. Both intensities have been normalised by their values at $E = -800$ meV and the chemical potential shift between two samples has been taken as $\delta\mu = 70$ meV.

We notice that due to a very sharp dependence on q of the matrix element in Eq.(2) any uncertainty of k_z does not smear out the strong dependence of $I_{im}(\mathbf{k}, E)$ on the in-plane momentum component, \mathbf{k}_{\parallel} . Averaging over k_z simply replaces $M(\mathbf{k} - \mathbf{g}, E)$ in Eq.(3) by

$$\tilde{M}(\mathbf{k}_{\parallel} - \mathbf{g}, E) \approx \frac{32c}{vm} \frac{(E + \Delta)^{5/2}}{[E + \Delta + (\mathbf{k}_{\parallel} - \mathbf{g})^2/m]^{7/2}} \rho_{im}(E + \Delta), \quad (4)$$

where c is the c -axis lattice constant. Also M and \tilde{M} can be very large for shallow impurity states, $M, \tilde{M} \gg 1/x$. Hence even the strong polaronic reduction of their weight, $Z \ll 1$, does not make band-tails invisible in ARPES at finite doping, in contrast to a complete reduction of the coherent band peak.

Since the chemical potential shifts towards the band edge with doping, Δ in Eqs.(3,4) becomes smaller. Hence, the band-tail peak, $I_{im}(\mathbf{k}, E)$, which is proportional to x , not only increases but also becomes sharper with doping as observed [2]. To provide more insight into the shape and momentum dependence of experimental EDC we approximate the band-tail DOS by the simple form, $\rho_{im}(E) = [n/\Gamma(p/n + 1/n)](E/\gamma)^p \exp(-E^n/\gamma^n)$, where $\Gamma(x)$ is the gamma-function. Exponents n, p depend on the dimensionality and the correlation length of the disorder potential: $n = 2$ both in 2D and 3D, $p = 2$ in 2D and $p = 7/2$ in 3D for the long range random potential correlations. In the short-range Gaussian-white-noise

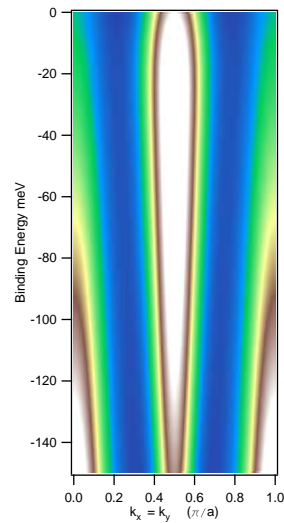


FIG. 3: Waterfall effect in the band-tail ARPES intensity (white colour corresponds to the highest intensity).

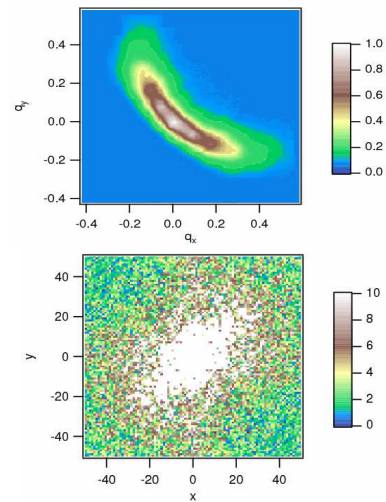


FIG. 4: Real space Fourier transform (lower panel) of the square root of ARPES intensities (arb. units) at the Fermi level in $\text{Ca}_{2-x}\text{Na}_x\text{CuO}_2\text{Cl}_2$ (upper panel, measured by Shen *et al.* [23] for $x = 0.12$) reveals the real-space size (in units of a) of localised in-gap states.

limit one obtains $n = 1, 1/2$ in 2D and 3D, respectively, and $p = 3/2$ in both dimensions [27]. We can separate impurity and band contributions by subtracting normalised ARPES intensity of the parent cuprate from the intensity of the doped one. Then, the band-tail ARPES, Eq.(4), fits well with the experimental relative intensities at all momenta around \mathbf{g} with $m = m_e$, $n = 2$, and $p = 7/2$, Fig.2. It describes the substantial loss of intensity with changing the momentum by only a few percent relative to \mathbf{g} , as well as the shape of the relative EDC.

We argue that band-tailing can also contribute to the waterfall effect. There are impurity tails near local maxima of the LDA+GTB valence band at Γ point $(0, 0)$ and at $\mathbf{g}_1 = (\pi/a, \pi/a)$, as shown in Fig.1. Different from in-gap impurity states at $\mathbf{g} = (\pi/2a, \pi/2a)$ these localised states are hybridised with the valence band states of the same energy (shown by stars in Fig.1). However, the hybridisation could be insignificant, if the corresponding matrix elements of the random potential are small due to a large momentum separation between those states of the order of $\pi/2a$. Hence, the impurity peaks reappear and disperse towards $(0, 0)$ and \mathbf{g}_1 at high binding energies, as observed in a number of doped cuprates [4, 5, 6, 7, 8, 9]. We illustrate the waterfall in Fig.3 by adding all three tail contributions, $I_{im}(\mathbf{k}, E) \propto n(E)[\tilde{M}(\mathbf{k}_{\parallel}, E+E_2) + \tilde{M}(\mathbf{k}_{\parallel} - \mathbf{g}, E) + \tilde{M}(\mathbf{k}_{\parallel} - \mathbf{g}_1, E+E_2)]$ where E_2 is roughly the valence band-width (we chose $E_2 = 500$ meV). We notice that the Fermi-Dirac distribution, $n(E)$, is replaced by its convolution with the Gaussian energy resolution function, $n(E) \rightarrow [1 - \text{erf}(E/\delta)]/2$ in plotting Figs.2,3 since the energy resolution $\delta = 20$ meV is much larger than $T \approx 2$ meV. Also the photoemission intensity comprises both band-tail and valence band contributions, so that the resulting dispersion could be different from the anomalous band-tail dispersion of relative intensities, Fig. 2.

Our theory proposes that the ARPES intensity near $(\pi/2a, \pi/2a)$ is proportional to the square of the Fourier component, $f_i(\mathbf{q})$, of the impurity wave-function envelope, Eq.(2). Therefore, we can find the real-space image of the function, $F_i(\mathbf{r})$, by taking the Fourier transform of the square root of the experimental intensities, Fig.4 (upper panel). Here we show the intensities

near the Fermi level measured in $\text{Ca}_{2-x}\text{Na}_x\text{CuO}_2\text{Cl}_2$ [23], which are very similar, if not identical to those in $\text{La}_{2-x}\text{Sr}_x\text{CuO}_4$ (compare Fig.1 [23] and Fig.2 in [2]). The real-space image (lower panel, Fig.4) reveals some band-mass anisotropy and the size of the localised state of about 20 lattice constants justifies the "envelope" approximation [26] used for the impurity wavefunction.

In summary, we have proposed an explanation for sharp "quasi-particle" peaks, "Fermi-arcs", and the high-energy waterfall in cuprates as a consequence of matrix-element effects of disorder-localised band-tails in the charge-transfer gap of doped Mott-Hubbard insulators. Importantly if holes are bound into bipolarons, the chemical potential remains within the single-particle band-tail at the bipolaron mobility edge even up to optimum doping, in agreement with $S - N - S$ tunnelling experiments [28] and insulating-like low-temperature resistivity of underdoped cuprates. In this case Δ in Fig.1 is half of the bipolaron binding energy [11], which is also the normal state pseudogap [29]. Recent scanning tunnelling microscopy at the atomic scale found intense nanoscale disorder in high-Tc superconductor $\text{Bi}_2\text{Sr}_2\text{CaCu}_2\text{O}_{8+\delta}$ [30] telling us that band-tailing indeed plays the important role in shaping single-particle spectral functions of doped Mott insulators.

We are grateful to ZX Shen and Tepei Yoshida for providing us with their raw ARPES data [2] and enlightening comments. We greatly appreciate valuable discussions with Arun Bansil, Sergey Borisenko, Ivan Bozovic, Jim Hague, Jan Jung, Alexander Kordyuk, Maxim Korshunov, Kyle Shen, and Jan Zaanen. This work was supported by EPSRC (UK) (grant number EP/C518365/1).

-
- [1] A. Damascelli, Z. Hussain and Zhi-Xun Shen, *Rev. Mod. Phys.* **75**, 473 (2003); X. J. Zhou *et al.*, *cond-mat/0604284*.
- [2] T. Yoshida *et al.*, *Phys. Rev. Lett.* **91**, 027001 (2003).
- [3] F. Ronning *et al.*, *Phys. Rev. B* **71**, 094518 (2005).
- [4] J. Graf *et al.*, *Phys. Rev. Lett.* **98**, 067004 (2007).
- [5] W. Meevasana *et al.*, *cond-mat/0612541*.
- [6] B. P. Xie *et al.*, *cond-mat/0607450*
- [7] Z.-H. Pan *et al.*, *cond-mat/0610442*.
- [8] J. Chang *et al.*, *cond-mat/0610880*.
- [9] A. A. Kordyuk *et al.*, *cond-mat/0702374*.
- [10] A. Macridin *et al.*, *cond-mat/0701429*.
- [11] A. S. Alexandrov and C. J. Dent, *Phys. Rev. B* **60**, 15414 (1999); A. S. Alexandrov and C. Sricheewin, *Europhys. Lett.* **58**, 576 (2002).
- [12] G. Wellein, H. Roder, and H. Fehske, *Phys. Rev. B* **53**, 9666 (1996)
- [13] A. S. Mishchenko and N. Nagaosa, *Phys. Rev. Lett.* **93**, 036402 (2004).
- [14] M. Hohenadler *et al.*, *Phys. Rev. B* **71**, 245111 (2005).
- [15] O. Rosch *et al.*, *Phys. Rev. Lett.* **95**, 227002 (2005).
- [16] J. P. Hague, *J. Phys.: Condens Matter* **15**, 2535 (2003).
- [17] E. G. Maksimov, O. V. Dolgov, and M. L. Kubic, *Phys. Rev. B* **72**, 212505 (2005).
- [18] S. V. Borisenko *et al.*, *Phys. Rev. Lett.* **96**, 117004 (2006).
- [19] M. Lindroos, S. Sahrakorpi, and A. Bansil, *Phys. Rev. B* **65**, 054514 (2002).
- [20] V. I. Anisimov, J. Zaanen, and O. K. Andersen, *Phys. Rev. B* **44**, 943 (1991).
- [21] S. G. Ovchinnikov *et al.*, *J. Phys.: Condens. Matter* **16**, L93 (2004); M. M. Korshunov *et al.*, *Phys. Rev. B* **72**, 165104 (2005).
- [22] N. P. Armitage *et al.*, *Phys. Rev. Lett.* **88**, 257001 (2002); K. M. Shen *et al.*, *Phys. Rev. B* **69**, 054503 (2004).
- [23] K. M. Shen *et al.*, *Science* **307**, 901 (2005).
- [24] K. M. Shen *et al.*, *Phys. Rev. B* **75**, 054503 (2007).
- [25] P. V. Mieghem, *Rev. Mod. Phys.* **64**, 755 (1992).
- [26] W. Kohn and J. M. Luttinger, *Phys. Rev.* **97**, 869-883 (1955).
- [27] B. I. Halperin and M. Lax, *Phys. Rev.* **148**, 722 (1966); R. Eymard and G. Duraffourg, *J. Phys. D: Appl. Phys.* **6**, 66 (1973); D. N. Quang and N. H. Tung, *Phys. Stat. Sol. B* **209**, 375 (1998).
- [28] I. Bozovic *et al.*, *Nature (London)* **422**, 873 (2003).
- [29] A. S. Alexandrov, in *Studies in High Temperature Superconductors*, ed. A.V. Narlikar (Nova Science Pub., NY

- 2006), **50**, pp. 1-69.
- [30] J. Lee *et al.*, Nature (London), **442** 546 (2006).